The sinking city: Earthquakes increase flood hazard in Christchurch, New Zealand

Matthew W. Hughes, *Dept. of Civil & Natural Resources Engineering, University of Canterbury, Private Bag 4800, Ilam, Christchurch, New Zealand;* ***Mark C. Quigley,*** *Dept. of Geological Sciences, University of Canterbury, Private Bag 4800, Ilam, Christchurch, New Zealand;* ***Sjoerd van Ballegooy, Bruce L. Deam,*** *Tonkin & Taylor Ltd, PO Box 5271, Wellesley Street, Auckland 1141, New Zealand;* ***Brendon A. Bradley,*** *Dept. of Civil & Natural Resources Engineering, University of Canterbury, Private Bag 4800, Ilam, Christchurch, New Zealand;* ***Deirdre E. Hart,*** *Dept. of Geography, University of Canterbury, Private Bag 4800, Ilam, Christchurch, New Zealand; and* ***Richard Measures,*** *National Institute of Water & Atmospheric Research (NIWA), PO Box 8602, Christchurch, New Zealand*

ABSTRACT

Airborne light detection and ranging (LiDAR) data were acquired over the coastal city of Christchurch, New Zealand, prior to and throughout the 2010 to 2011 Canterbury Earthquake Sequence. Differencing of pre- and post-earthquake LiDAR data reveals land surface and waterway deformation due to seismic shaking and tectonic displacements above blind faults. Shaking caused floodplain subsidence in excess of 0.5 to 1 m along tidal stretches of the two main urban rivers, greatly enhancing the spatial extent and severity of inundation hazards posed by 100-year floods, storm surges, and sea-level rise. Additional shaking effects included river channel narrowing and shallowing, due primarily to liquefaction, and lateral spreading and sedimentation, which further increased flood hazard. Differential tectonic movement and associated narrowing of downstream river channels decreased channel gradients and volumetric capacities and increased upstream flood hazards. Flood mitigation along the large regional Waimakariri River north of Christchurch may have, paradoxically, increased the long-term flood hazard in the city by halting long-term aggradation of the alluvial plain upon which Christchurch is situated. Our findings highlight the potential for moderate magnitude (MW 6–7) earthquakes to cause major topographic changes that influence flood hazard in coastal settings.

INTRODUCTION

Approximately 10% of the world's population inhabits low-lying (≤10 m above sea level) coastal areas, and most of this population is contained within densely populated urban centers (McGranahan et al., 2007). Cities constructed on low-lying coastal and river plains are highly vulnerable to ocean-sourced hazards (e.g., sea-level rise, storm surges, tsunamis) and terrestrial hazards (e.g., surface subsidence and compaction, flooding, erosion, sediment supply changes, groundwater table changes) induced by natural and/or anthropogenic processes (Syvitski et al., 2009; Nicholls and Cazenave, 2010). Coastal population growth and concentration, economic development, and urbanization are expected to greatly increase exposure and loss to the impacts of relative sea-level rise (Nicholls and Cazenave, 2010; IPCC, 2014) and coastal flooding (Hanson et al., 2011; Hallegatte et al., 2013) through the next century, defining one of society's greatest challenges. Geospatial data, such as satellite-based synthetic aperture radar and airborne light detection and ranging (LiDAR), are increasingly being used to measure surface subsidence and delineate areas prone to flood and sea-level rise hazards (Dixon et al., 2006; Wang et al., 2012; Webster et al., 2006), thereby assisting land-use planning and management decisions (Brock and Purkis, 2009).

Great (MW ≥ 8.5) earthquakes on subduction zones may cause abrupt and dramatic elevation changes to coastal environments. The 1964 MW 9.0 Alaska earthquake caused tidal marshes and wetlands to subside up to 2 m (Shennan and Hamilton, 2006); the 2005 MW 8.7 Nias earthquake caused up to 3 m in coastal uplift proximal to the trench and 1 m of more distal coastal subsidence (Briggs et al., 2006); and the 2011 MW 9.0 Tohoku earthquake caused subsidence up to 1.2 m along the Pacific Coast of northeastern Japan (Geospatial Information Authority of Japan, 2011, cited in IPCC, 2014). However, the influence of moderate magnitude (i.e., MW 6–7) earthquakes, which can occur in both interplate and intraplate settings, on coastal flood and sea-level hazards is not well characterized and not typically included in studies that assess the future vulnerability of coastal populations (McGranahan et al., 2007).

In this paper, we summarize differential vertical and horizontal ground movements in Christchurch, New Zealand, using airborne LiDAR survey data captured prior to, during, and after the 2010 to 2011 Canterbury Earthquake Sequence (CES). Differential LiDAR applications in earthquake studies have been used to map deformation along fault zones (e.g., Duffy et al., 2013; Oskin et al., 2012); however, this is the first differential LiDAR study showing the cumulative surface effects of earthquake shaking and faulting on an urban environment. Here we show that earthquakes sourced from blind and/or previously unrecognized faults, in addition to those from known seismic sources, have the ability to create profound landscape changes that impact current and future flood hazards associated with urban rivers and relative sea-level

GSA Today, v. 25, no. 3–4, doi: 10.1130/GSATG221A.1.

E-mails: Hughes: matthew.hughes@canterbury.ac.nz; Quigley: mark.quigley@canterbury.ac.nz; Ballegooy: svanballegooy@tonklin.co.nz; Deam: BDeam@tonklin.co.nz; Bradley: brendon.bradley@canterbury.ac.nz; Hart: deirdre.hart@canterbury.ac.nz; Measures: richard.measures@niwa.co.nz.

rise. We also highlight the complex interactions within coexisting natural and built environments, where anthropogenic activities designed to mitigate regional flood hazard may deprive subsiding coastal areas of replenishing sediment that would have provided natural mitigation of coastal and flooding hazards.

GEOLOGY AND GEOMORPHOLOGY OF CHRISTCHURCH, NEW ZEALAND

Christchurch (population ~350,000 at latest census) is located on the eastern coast of New Zealand's South Island, adjacent to the Pacific Ocean. Previously a seasonal resource-gathering area for Maori, development of the built environment began with English colonial settlement in the 1850s. Most of the city resides upon late Quaternary alluvial sediments derived from Mesozoic quartzo-feldspathic metasediments (graywackes and argillites) in source catchments in the Southern Alps. The city is bounded to the south by Banks Peninsula, comprised largely of Neogene volcanic rocks, and to the north by the large, braided Waimakariri River. Two smaller spring-fed tidally influenced rivers, the Avon and Heathcote, flow through the city into the Avon-Heathcote Estuary and out to Pegasus Bay via an inlet to the south (Fig. 1).

Following the last deglaciation, marine transgression reached its furthest inland extent ~10 km west of the modern coastline ca. 6.5 ka (Brown and Weeber, 1992). Since 6.5 ka, the coastline in the vicinity of central Christchurch has prograded through episodic coastal and alluvial deposition, fed by sediments from the continental shelf and Waimakariri River. Basher et al. (1988) give a comprehensive geomorphologic overview of Waimakariri alluvial fan evolution over the Holocene. The lower floodplain comprises a set of nested alluvial fans with each fanhead lower and farther downstream than the previous one. Fan-building occurred in response to channel incision of older fans upstream and by sediment from basin headwaters. Significant river avulsion has occurred periodically as a result of river sediment bed-load overtopping natural channel levees, leading to the river mouth using the Avon-Heathcote Estuary at least several times over the past 6.5 ka. This includes avulsion north and south of Banks Peninsula several times through the Holocene, with the latest northward migration commencing in the last millennium (Soons et al., 1997; McFadgen and Goff, 2005) (Fig. 1). The co-evolution of floodplain and coastal landscapes produced significant spatial heterogeneity in Holocene sediments underlying Christchurch, with alluvial gravels dominating the west of the city and coastal dunes and estuarine/tidal wetland sediments dominating the east, with finer alluvial overbank deposits from the Avon and Heathcote Rivers superimposed on these accumulations (Brown and Weeber, 1992).

Pre-CES subsidence rates across Christchurch are poorly constrained, but the dominant processes would have been long-term sediment loading and periodic settling through local and regional earthquakes. Minimum earthquake peak ground accelerations (PGA) required to initiate liquefaction manifestations at the ground surface and surface subsidence (0.1–0.2 g) have estimated return periods of 40 to 170 years for Christchurch shallow soil sites (Stirling et al., 2008). A local earthquake (M_W 4.7–4.9) in 1869 caused pervasive damage in parts of Christchurch consistent with PGA ≥0.2 g shaking (Downes and Yetton, 2012) and may have caused surface subsidence; it was reported after the earthquake that "the tide runs higher up the Heathcote River than formerly" (Weekly News, 26 June 1869).

Subsidence in the Christchurch region has been counteracted over geological time scales by sediment delivery from Waimakariri

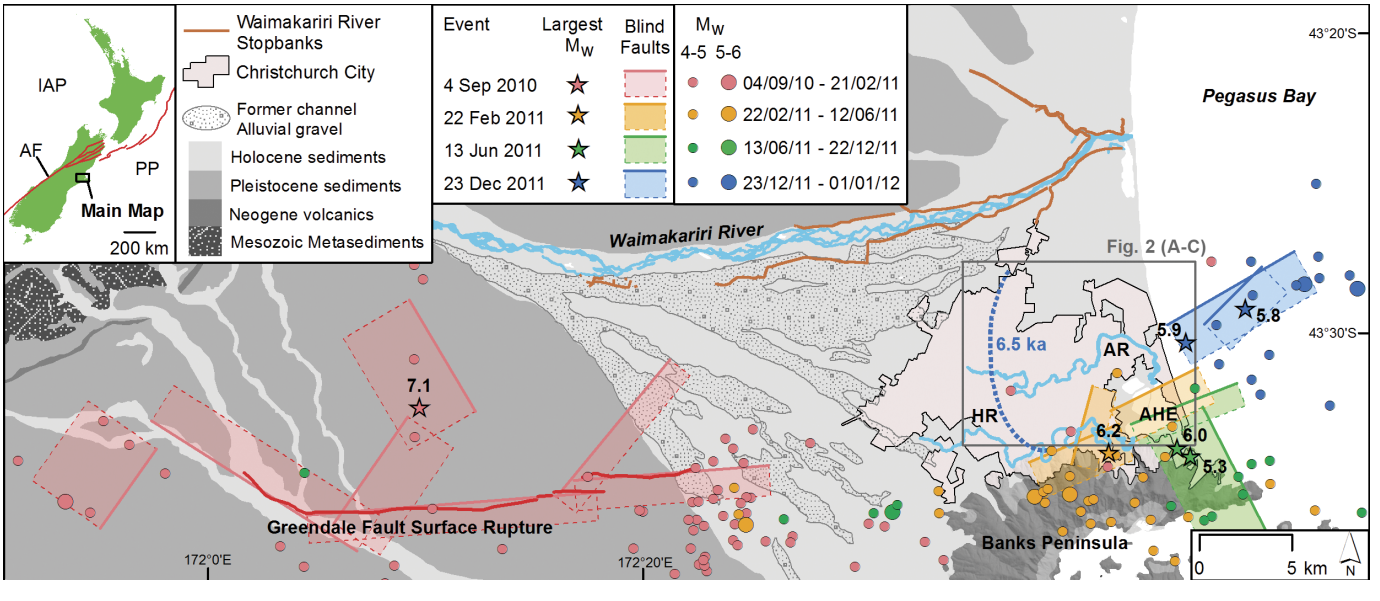

Figure 1. Geologic and seismic context of Christchurch through the 2010–2011 Canterbury Earthquake Sequence (CES). Shown are inferred causative fault planes and associated largest moment magnitudes (M_W) for events on 4 Sept. 2010, 22 Feb. 2011, 13 June 2011, and 23 Dec. 2011. Also shown are M_W 4–6 epicenters in the months following each major event. The Greendale Fault surface rupture coincident with the 4 Sept. 2010 events is shown, after Quigley et al. (2012). Also shown are the Waimakariri River with adjacent stopbanks and former channel locations evidenced by alluvial gravels, Avon River (AR), Heathcote River (HR), and Avon-Heathcote Estuary (AHE). The blue dashed line is the 6.5-ka maximum inland extent of postglacial marine transgression, after Brown and Weeber (1992). Inset map shows location of the study region in New Zealand, the Alpine Fault (AF), and wider tectonic boundary (red lines) between the Indo-Australian plate (IAP) and Pacific plate (PP).

avulsions. This natural sediment replenishment entails the rapid advance of coarse alluvium along relict and newly excavated channels, driven by high river flows and accompanied by extensive flooding. Such avulsions pose a severe physical threat to the built environment. Extensive flood protection works, including gravel extraction, were first established in 1928, with three subsequent flood events breaching the primary stopbank (levee) system, resulting in floodplain inundation. Throughout the majority of European settlement, the city has been spared from major floods from the Waimakariri, although stopbank failure remains a hazard. Christchurch has also long been vulnerable to localized flooding from its urban rivers, exacerbated by low-lying, relatively flat terrain with low gradients and high groundwater levels, extreme tides, and storm surge. Urban expansion since the 1880s imparted distinct anthropogenic signatures on local hydrology. Widespread drainage works undertaken for urban development caused ground surface subsidence due to reduction of the groundwater levels, leading to historical surface flooding and ponding in low-lying areas. In parallel, separate underground storm water and waste water systems were established, with the latter long recognized as being "leaky"—that is, allowing infiltration into pipes with associated draining of groundwater and suppression of local water tables (Wilson, 1989). The storm water system, originally integrating open channels and buried pipes and then incorporating roadside gutters, was developed to manage overland flow runoff exacerbated by expansion of impermeable surfaces through suburban development.

THE CES AND URBAN LANDSCAPE EVOLUTION

Between September 2010 and December 2011, Christchurch was damaged by six earthquakes: 4 Sept. 2010 (M_W = 7.1); 22 Feb. 2011 (M_W = 6.2, 185 fatalities); 13 June 2011 (two earthquakes: M_W = 5.3 at 1 p.m. and M_W = 6.0 at 2:20 p.m.) and 23 Dec. 2011 (two earthquakes: M_W = 5.8 at 1:58 p.m. and M_W = 5.9 at 3:18 p.m.) (Fig. 1; for detailed reviews of the geologic and seismic aspects of the CES, see Beavan et al., 2010, 2011, 2012a, 2012b; Duffy et al., 2013; Quigley et al., 2012; Bradley et al., 2014). The close proximity of causative faults to Christchurch generated strong ground motions (Bradley and Cubrinovski, 2011; Bradley, 2012) that caused extensive damage to residential and commercial properties (Bech et al., 2014; Fleischman et al., 2014; Moon et al., 2014) and infrastructure lifelines, particularly potable water, waste water, and road networks (Cubrinovski, et al., 2014a, 2014b, 2014c; O'Rourke et al., 2014). Much of the damage to the city's built environment was caused by widespread soil liquefaction that occurred predominantly in saturated, unconsolidated alluvial and marine fine sediments in east Christchurch, in the region of late Holocene coastal progradation. In susceptible soils with high water tables (e.g., suburbs adjacent to the Avon River), liquefaction was manifested at the ground surface in earthquakes as low as M_W 5.0 and PGAs as low as 0.08 g (Quigley et al., 2013). Less-susceptible soils required higher shaking intensities for liquefaction initiation (Tonkin & Taylor, 2013; van Ballegooy et al., 2014b). Liquefaction caused significant ground deformations, ejection of groundwater and sediments on to the ground surface, and lateral spread around rivers (Cubrinovski et al., 2014c; Quigley et al., 2013; Green et al., 2014; van Ballegooy et al., 2014b). In some areas, loadings from structures and preferential ejecta pathways through roads and buried infrastructure imparted distinct anthropogenic signatures on surface ejecta patterns.

In 2003, the Christchurch City Council commissioned an aerial LiDAR survey for hydrological modeling purposes. Following the 4 Sept. 2010 Darfield earthquake, another LiDAR survey was commissioned and flown on 5 Sept. 2010 by the New Zealand Ministry of Civil Defense and Emergency Management to quantify property subsidence and to facilitate insurance assessments and reconstruction work. Further LiDAR campaigns were flown typically one month after each subsequent major CES earthquake to provide time for ejected sand and silt to be removed from most properties and streets, so that measurements recorded ground surface level. LiDAR capture equipment had a horizontal accuracy of 0.44 to 0.55 m, with a vertical accuracy of ±0.15 m for the 2003 survey and ±0.07 m for the post-earthquake surveys. These errors exclude Global Positioning System network error and approximations within the New Zealand Quasigeoid 2009 reference surface, which has an expected vertical accuracy of ±0.07 m. From each LiDAR dataset a bare-earth 5-m-resolution Digital Elevation Model (DEM) was generated; the 5-m-resolution was determined to be optimal for interpolation of pre- and post-earthquake LiDAR ground returns in the urban environment. The accuracy of LiDAR data and bare-earth DEMs were assessed against reference geodetic survey control benchmarks and topographic surveys conducted pre-CES on roads and subdivisions at suburb-level in August 2011 and on residential properties in January 2012. These assessments showed reasonable accuracy as a whole, with hard surfaces providing smaller standard deviations of errors for roads than for residential properties, reflecting the differing roughness of the two types of terrain. Here we show total vertical elevation changes (ΔE_{Tot}), elevation changes due to liquefaction (ΔE_{Liq}), lateral ground movements due to liquefaction (ΔX_{Liq}), and vertical tectonic changes (ΔE_{Tec}) (Fig. 2). Tectonic movements were determined using satellite interferometry synthetic aperture radar data (see Beavan et al., 2011, 2012b), which we subtracted from ΔE_{Tot} as determined by LiDAR-derived DEMs to produce ΔE_{Liq}.

We also present pre-/post-earthquake differential elevation analysis (ΔE_{Tot}) for the Avon-Heathcote Estuary, based on 1-m-resolution DEMs interpolated from LiDAR data (area of bed exposed above water surface during survey), supplemented by ground survey and depth-sounder survey data for areas covered by estuarine waters during LiDAR surveys (Measures et al., 2011; Measures and Bind, 2013). Pre-/post-earthquake ground surveys and echo-sounder surveys were conducted using Real-Time Kinetic Global Navigation Satellite System positioning, on foot or with a boat-mounted depth sounder, and calibrated to local benchmarks.

The 4 September 2010 Darfield earthquake caused 74% of central and eastern Christchurch to subside; 60% of this area subsided up to 0.2 m (Fig. 2A). Vertical tectonic displacements of 0.8 to 1.8 m along the associated surface rupture ~50 km west of Christchurch caused partial river avulsion and flooding (Duffy et al., 2013). The 22 February 2011 Christchurch earthquake caused 83% of eastern and central Christchurch to subside further; 78% subsided up to 0.3 m, with localized areas exceeding 1 m. This event also caused a clear signature of tectonic uplift (~0.45 m) around the Avon-Heathcote Estuary caused by blind faults (Fig. 2A and 2E). Compared to pre-earthquake elevations, 86% of central and eastern Christchurch subsided through the CES; 10% subsided more than 0.5 m, with some localized locations exceeding 1 m. Cumulative tectonic subsidence through the CES reached 0.18 m (Fig. 2E). Both

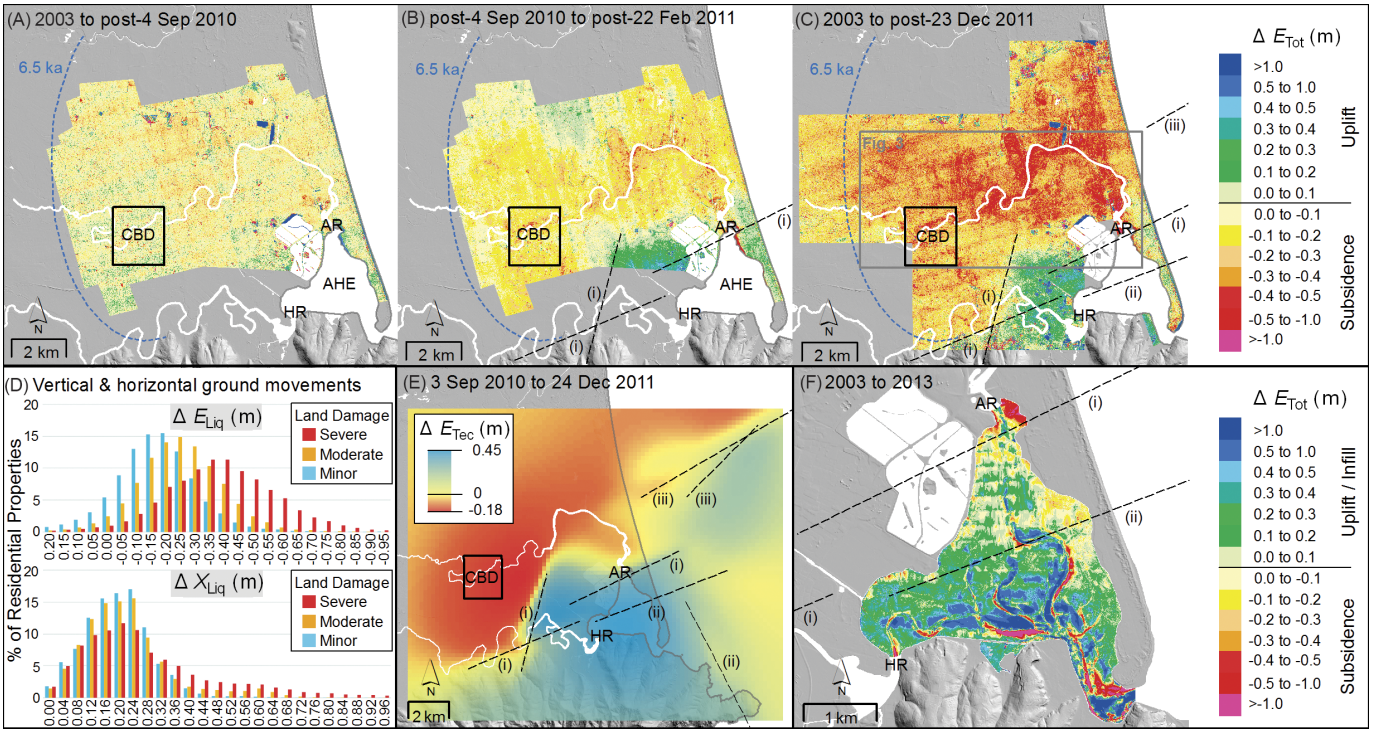

Figure 2. (A–C) Differential LiDAR models illustrating total vertical ground movements (ΔE_{Tot}) in Christchurch through the Canterbury Earthquake Sequence (CES). (A) Vertical movement from the initial 4 Sept. 2010 event. (B) Further vertical movement resulting from the 22 Feb. 2011 event. (C) Total vertical movements through the entire CES. Also shown are location of Avon River (AR) and Heathcote River (HR) mouths, the Avon-Heathcote Estuary (AHE), the Central Business District (CBD), the 6.5-ka maximum inland extent of postglacial marine transgression (blue dashed line) after Brown and Weeber (1992), and blind fault locations (black dashed lines) for 22 Feb. 2011 (i), 13 June 2011 (ii), and 23 Dec. 2011 (iii). Linear artefacts evident in (A)–(C) are due to minor elevation errors along LiDAR flight lines. (D) Histograms of LiDAR vertical (ΔE_{Liq}) and horizontal (ΔX_{Liq}) displacements classified according to observed land damage classes: ΔE_{Liq} was calculated by subtracting tectonic vertical movements (Beavan et al., 2012b) from ΔE_{Tot}. (E) Cumulative tectonic vertical movements (ΔE_{Tec}) through the CES, with blind fault locations shown. (F) Cumulative vertical movements through the CES for the AHE (ΔE_{Tot}), with blind fault locations shown. Note that linear artefacts in (F) are due to minor elevation errors due to interpolation between ground survey and depth-sounder survey transects.

vertical and horizontal ground movements evident in LiDAR-derived DEMs correlated strongly with detailed ground-based land damage observations conducted by Tonkin & Taylor Ltd. for New Zealand Earthquake Commission insurance assessments (Fig. 2D). Horizontal ground movements were recorded across the city, and areas adjacent to the Avon River experienced severe lateral spread, particularly on current and former inner meander bends and tidal wetland sediments, in places exceeding 2 m (Beavan et al., 2012a) (Fig. 3). A comparison of pre-CES and post–13 June 2011 river and floodplain cross sections, derived from a combination of direct river bed depth measurements and LiDAR data, shows floodplain subsidence and river channel narrowing and shallowing (Fig. 3, inset panels i–v) resulting from lateral spread and sedimentation from liquefaction ejecta entering waterways. Smaller cross-sectional channel areas and lower flood plains collectively reduced channel cross-sectional areas and increased flood hazard. The upper reaches of the Heathcote River are located in an area of net tectonic subsidence through the CES, and its lower reaches are in an area of uplift (Fig. 2E) that reduced river gradients. Differential elevation analysis for the Avon-Heathcote Estuary (Fig. 2F) shows that 76% of its area was uplifted during the CES, 60% of the area is in the 0–0.4 m uplift range corresponding to the cumulative CES tectonic signature, and subsidence >1 m at the Avon River mouth results from combined tectonic down-throw and liquefaction/lateral spread (Fig. 2F). In other areas, Avon-Heathcote Estuary subsidence of more than 1 m reflects natural widening or deepening of estuarine tidal channels since pre-CES surveys, and comparable upward movements reflect channel infilling. Using a calibrated hydrodynamic model (Measures and Bind, 2013), neap and spring tidal prism volumes are calculated to have reduced by 17.6% and 12.4%, respectively, with an average tidal prism reduction of 14.6%.

EARTHQUAKES, FLOODING, AND SEA-LEVEL RISE: THE PRESENT AND FUTURE

Prior to the CES, flooding was perceived as Christchurch's primary hazard (Center for Advanced Engineering, 1995). Contributors included urban rivers and streams, localized ponding of overland flow on the developed coastal plain, and drainage-induced ground settlement. In 2010 to 2011, seismically induced landscape changes significantly increased the city's flood risk. Key factors in this increase were the widespread tectonic and liquefaction-induced subsidence and alteration of the longitudinal and cross-sectional profiles and sediment regimes of urban waterways. Lowering of surface elevations relative to water tables (van Ballegooy et al., 2014a) is likely to have increased the liquefaction and flood hazard. With groundwater levels (i.e., fully saturated soils) now closer to the ground surface, there is less soil above the

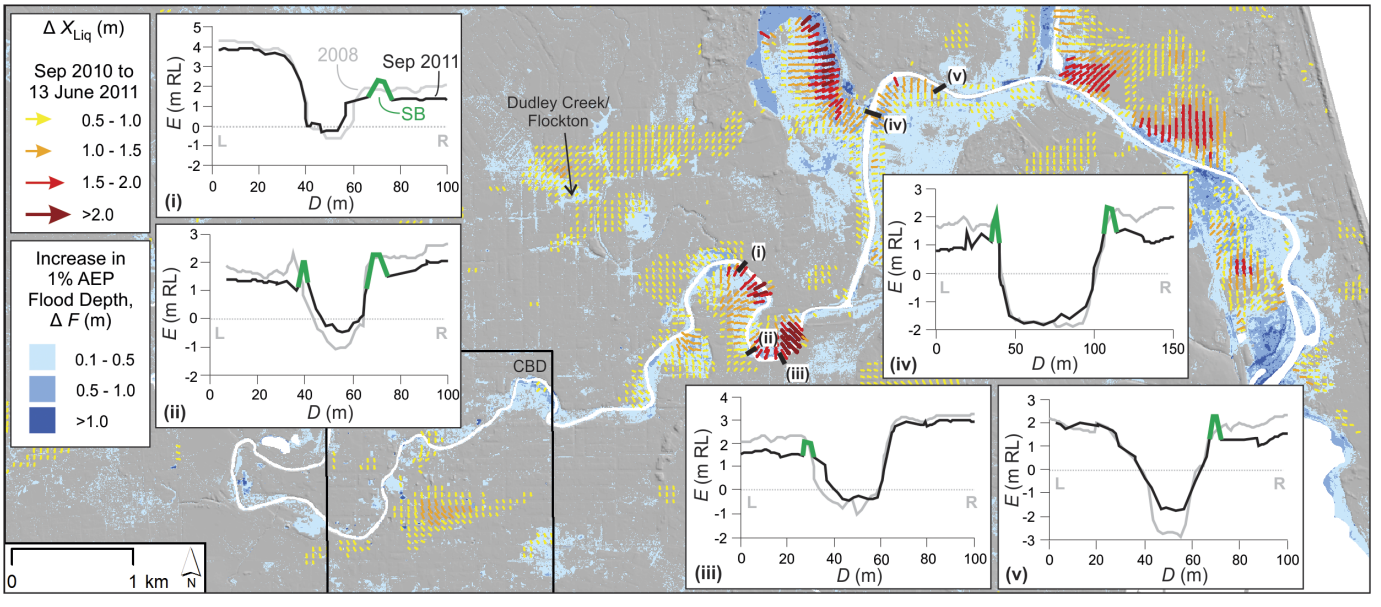

Figure 3. Main map: Cumulative horizontal movements (ΔX_{Liq}) in Christchurch in the vicinity of the Avon River from Sept. 2010 to 13 June 2011, derived from LiDAR offset analysis (Beavan et al., 2012a). Also shown: Increased 1-in-100-year storm event (1% Annual Exceedence Probability [AEP]) flood depths (ΔF) due to subsidence caused by the Canterbury Earthquake Sequence using current sea level, rainfall, and urban extent. The Christchurch Central Business District (CBD) is shown, as is the Dudley Creek/Flockton area where recent flooding of residential properties has been problematic. Inset panels: Floodplain and river cross sections (i–v) obtained from field survey and LiDAR analyses, with elevation (E) changes shown as relative level in meters (m RL) from 2008 (solid gray lines) to Sept. 2011 (black lines). Transect distance (D) is in meters (m). The locations of stopbanks (SB) constructed after the 22 Feb. 2011 Christchurch earthquake are shown in green.

water table and therefore less capacity to absorb water during storm events. Leakage of underlying artesian aquifers through breached aquitards may also have influenced local hydrologic conditions (Cox et al., 2012) and thus impacted on surface water infiltration. Another significant contributor to the increased flood hazard is widespread earthquake damage of the urban storm water network, much of which is yet to be repaired, including open channels and underground pipes that were compromised by breakages, liquefaction blockages, and gradient changes. The post-earthquake flood-scape may also have been influenced by New Zealand statutory resource management framework changes, instituted in the early 1990s, which were locally translated into a new approach of naturalizing urban waterways and reducing engineered river widening and dredging programs. Pre-1990s development of the urban floodplains that are now experiencing enhanced flood hazards was facilitated by the earlier engineering approach to the urban rivers (Canterbury Regional Council, 1993, 1997; Wilson, 1989).

In 2013, the Christchurch City Council released revised flood extents for projected 1-in-50-yr and 1-in-200-yr rainfall events using post-earthquake LiDAR-derived DEMs (CCC, 2014). The city subsequently experienced several intensive rainstorms in March 2014, resulting in widespread flooding of properties in river suburbs that in some instances exceeded historical flooding depths and spatial extents due to floodplain subsidence through the CES. Although the 1-in-50-yr models were good predictors of flooding at higher elevations, they over-predicted coastal flooding because they incorporated a future 0.5 m increase in relative sea level, a 16% increase in annual rainfall, and maximum probable urban development impacts on storm water runoff. Here we present the latest assessments of increased flood depths for a 1-in-100-yr event based on current sea level, rainfall, and urban development (Fig. 3). These flood depths were modeled using independent hydraulic modeling for watercourses and rain-on-grid for overland flows based on pre- and post-CES DEMs; our ongoing research is assessing the ability of these models to quantitatively hindcast the March 2014 flooding. The documentation of large, loss-inducing flood events following the CES has prompted an urgent and intent governmental focus on appropriate infrastructure and urban planning responses; at present, the city's post-quake flood-scape is cited as the primary concern of city authorities.

Relative sea-level rise of 0.5 to 1 m occurred in suburbs adjoining the lower Avon River and Avon-Heathcote Estuary that experienced tectonic down-throw and significant liquefaction/lateral spread subsidence through the CES. These areas have thus experienced the equivalent of several centuries of projected relative sea-level rise in the absence of land elevation changes at the current global rate of sea-level rise of 3.3 ± 0.4 mm yr^{-1} (Cazenave et al., 2014) and thus provide useful analogues for the potential impacts of sea-level rise in other settings globally. In this instance, gravel stop-banks were constructed along much of the Avon River in 2011 to temporarily mitigate the post-earthquake flood hazard (Fig. 3, inset panels i–v). More thorough measures are required, including locally tailored cost-benefit analyses of climate adaptation options (e.g. Aerts et al., 2014) and investigative analysis of urban wetlands e,cosystems (Kirwan and Megonigal, 2013) and their potential role in soft-engineering flood mitigation (Temmerman et al., 2013). Probabilistic approaches that consider future impacts from natural phenomena, including tropical and extra-tropical cyclones (Woodruff et al., 2013), earthquakes (Gerstenberger et al., 2014), and liquefaction (Quigley et al., 2013),

are important. Investigations addressing the dynamic geomorphic responses of urban rivers and coastal plains to relative sea-level rise, shoreline retreat, groundwater responses, liquefaction, subsidence, and coastal aquifer resources are all urgently required. In parallel with these scientific considerations, there also needs to be a focus on how current policies, planning, and socio-economic contexts will influence trajectories of urban form, and to what degree these will influence the exposure of current and future communities to continued flooding and sea-level rise.

The anthropogenic intervention of long-term geologic processes that previously enabled sediment aggradation to rebuild topography in this area means that subsidence will continue to dominate the topographic evolution of Christchurch. Similar scenarios, where prograding sediment has been diverted from subsiding areas, are likely to plague coastal settlements worldwide. Strong earthquakes sourced from previously unidentified and/or blind faults and their impacts on flood and relative sea levels add to the myriad of short- to long-term challenges facing coastal environments throughout the world.

Future investigations of the impacts of relative sea-level rise on coastal populations should consider the role of earthquakes, including those that may be sourced from unknown and/or proximal faults, in reshaping coastal topography and thus influencing the dynamics of coastal and flood hazards. As shown here, this is particularly important for densely populated, low-lying, and tectonically active regions built upon youthful and liquefiable alluvial and marine sediments.

ACKNOWLEDGMENTS

We thank the New Zealand Earthquake Commission for research capability funding and for provision of LiDAR data. These and other data are available on the Canterbury Geotechnical Database (https://canterburygeotechnicaldatabase.projectorbit.com/). We also thank Environment Canterbury and the New Zealand Ministry of Business, Innovation and Employment (MBIE contract UOCX0902) for funding analyses of the Avon-Heathcote Estuary.

REFERENCES CITED

Aerts, J.C.J.H., Botzen, W.J.W., Emanuel, K., Lin, N., and De Moel, H., 2014, Evaluating flood resilience strategies for coastal megacities: Science, v. 344, p. 473–475, doi: 10.1126/science.1248222.

Basher, L.R., Hicks, D.M., McSaveny, M.J., and Whitehouse, I.E., 1988, The lower Waimakariri River floodplain: A geomorphological perspective: A report for North Canterbury Catchment Board, 33 p.

Beavan, J., Samsonov, S., Motagh, M., Wallace, L., Ellis, S., and Palmer, N., 2010, The Darfield (Canterbury) Earthquake: Geodetic observations and preliminary source model: Bulletin of the New Zealand Society for Earthquake Engineering, v. 43, p. 228–235.

Beavan, J., Fielding, E., Motagh, M., Samsonov, S., and Donnelly, N., 2011, Fault location and slip distribution of the 22 February 2011 M_W 6.2 Christchurch, New Zealand, Earthquake from geodetic data: Seismological Research Letters, v. 82, p. 789–799, doi: 10.1785/gssrl.82.6.789.

Beavan, J., Levick, S., Lee, J., and Jones, K., 2012a, Ground displacements and dilational strains caused by the 2010–2011 Canterbury earthquakes: GNS Science Consultancy Report 2012/67.59, https://canterburygeotechnicaldatabase.projectorbit.com (last accessed 12 Dec. 2014).

Beavan, J., Motagh, M., Fielding, E.J., Donnelly, N., and Collett, D., 2012b, Fault slip models of the 2010–2011 Canterbury, New Zealand, earthquakes from geodetic data and observations of postseismic ground deformation: New Zealand Journal of Geology and Geophysics, p. 37–41, doi: 10.1080/00288306.2012.697472.

Bech, D., Cordova, P., Tremayne, B., Tam, K., Weaver, B., Wetzel, N., Parker, W., Oliver, L., and Fisher, J., 2014, Common structural deficiencies identified in Canterbury buildings and observed versus predicted performance: Earthquake Spectra, v. 30, p. 335–362, doi: 10.1193/021513EQS028M.

Bradley, B.A., 2012, Strong ground motion characteristics observed in the 4 September 2010 Darfield, New Zealand earthquake: Soil Dynamics and Earthquake Engineering, v. 42, p. 32–46, doi: 10.1016/j.soildyn.2012.06.004.

Bradley, B.A., and Cubrinovski, M., 2011, Near-source strong ground motions observed in the 22 February 2011 Christchurch Earthquake: Seismological Research Letters, v. 82, no. 6, p. 853–865, doi: 10.1785/gssrl.82.6.853.

Bradley, B.A., Quigley, M.C., Van Dissen, R.J., and Litchfield, N.J., 2014, Ground motion and seismic source aspects of the Canterbury Earthquake Sequence: Earthquake Spectra, v. 30, p. 1–15, doi: 10.1193/030113EQS060M.

Briggs, R.W., Sieh, K., Meltzner, A.J., Natawidjaja, D., Galetzka, J., Suwargadi, B., Hsu, Y.-J., Simons, M., Hananto, N., Suprihanto, I., Prayudi, D., Avouac, J.-P., Prawirodirdjo, L., and Bock, Y., 2006, Deformation and slip along the Sunda megathrust in the great 2005 Nias-Simeulue earthquake: Science, v. 311, p. 1897–1901, doi: 10.1126/science.1122602.

Brock, J.C., and Purkis, S.J., 2009, The emerging role of LiDAR remote sensing in coastal research and resource management: Journal of Coastal Research, Special Issue 53, p. 1–5, doi: 10.2112/SI53-001.1.

Brown, L.J., and Weeber, J.H., 1992, Geology of the Christchurch Urban Area: GNS Science, scale 1:25:000, 104 p.

Canterbury Regional Council, 1993, Avon and Heathcote catchment, rivers and estuary: Issues and options for managing the Heathcote River floodplain: Canterbury Regional Council Report R93(1), 43 p.

Canterbury Regional Council, 1997, Avon River: Issues and options for managing the Avon River floodplain: Canterbury Regional Council Report R97(1), 41 p.

Cazenave, A., Dieng, H., Meyssignac, B., Von Schuckmann, K., Decharme, B., and Berthier, E., 2014, The rate of sea-level rise: Nature Climate Change, v. 4, p. 358–361, doi: 10.1038/nclimate2159.

CCC, 2014, Flood extent models, Christchurch city council flood modeling data, hosted by the Canterbury Earthquake Recovery Authority: http://maps.cera.govt.nz/advanced-viewer/?Viewer=Ccc-Floor-Levels (last accessed 12 Dec. 2014).

Center for Advanced Engineering, 1995, Risks and Realities—A Multidisciplinary Approach to the Vulnerability of Lifelines to Natural Hazards: Report of the Christchurch Engineering Lifelines Group: Christchurch, New Zealand, University of Canterbury, Center for Advanced Engineering, 312 p.

Cox, S.C., Rutter, H.K., Sims, A., Manga, M., Weir, J.J., Ezzy, T., White, P.A., Horton, T.W., and Scott, D., 2012, Hydrological effects of the M_W 7.1 Darfield (Canterbury) earthquake, 4 September 2010: New Zealand Journal of Geology and Geophysics, v. 55, no. 3, p. 231–247, doi: 10.1080/00288306.2012.680474.

Cubrinovski, M., Hughes, M., Bradley, B., Noonan, J., Hopkins, R., McNeill, S., and English, G., 2014a, Performance of horizontal infrastructure in Christchurch City through the 2010–2011 Canterbury Earthquake Sequence: University of Canterbury, Civil & Natural Resources Engineering Research Report 2014-02, March 2014, 129 p.

Cubrinovski, M., Hughes, M., and O'Rourke, T., 2014b, Impacts of liquefaction on the potable water system of Christchurch in the 2010–2011 Canterbury (NZ) earthquakes: Journal of Water Supply: Research & Technology–Aqua, v. 63, p. 95–105, doi: 10.2166/aqua.2013.004.

Cubrinovski, M., Winkley, A., Haskell, J., Palermo, A., Wotherspoon, L., Robinson, K., Bradley, B., Brabhaharan, P., and Hughes, M., 2014c, Spreading-induced damage to short-span bridges in Christchurch: Earthquake Spectra, v. 30, p. 57–83, doi: http://dx.doi.org/10.1193/030513EQS063M.

Dixon, T.H., Amelung, F., Feretti, A., Novali, F., Rocca, F., Dokka, R., Sella, G., Kim, S.-W., Wdowinski, S., and Whitman, D., 2006, Subsidence and flooding in New Orleans: Nature, v. 441, p. 587–588, doi: 10.1038/441587a.

Downes, G., and Yetton, M., 2012, Pre-2010 historical seismicity near Christchurch, New Zealand: The 1869 M_W 4.7–4.9 Christchurch and 1870 M_W 5.6–5.8 Lake Ellesmere earthquakes: New Zealand Journal of Geology and Geophysics, v. 55, no. 3, p. 199–205, doi: 10.1080/00288306.2012.690767.

Duffy, B., Quigley, M., Barrell, D.J.A., van Dissen, R., Stahl, T., Leprince, S., McInnes, C., and Bilderback, E., 2013, Fault kinematics and surface deformation across a releasing bend during the 2010 M_W 7.1 Darfield, New Zealand, earthquake revealed by differential LiDAR and cadastral surveying: GSA Bulletin, v. 125, p. 420–431, doi: 10.1130/B30753.1.

Fleischman, R.B., Restrepo, J.I., Pampanin, S., Maffei, J.R., Seeber, K., and Zahn, F.A., 2014, Damage evaluations of precast concrete structures in the 2010–2011 Canterbury Earthquake Sequence: Earthquake Spectra, v. 30, p. 277–306, doi: 10.1193/031213EQS068M.

Geospatial Information Authority of Japan, 2011, Crustal movements in the Tohoku District, Rept. CCEP, v. 86, p. 184–272.

Gerstenberger, M., McVerry, G., Rhoades, D., and Stirling, M., 2014, Seismic hazard modeling for the recovery of Christchurch: Earthquake Spectra, v. 30, no. 1, p. 17–29, doi: 10.1193/021913EQS037M.

Green, R.A., Cubrinovski, M., Cox, B., Wood, C., Wotherspoon, L., Bradley, B., and Maurer, B., 2014, Select liquefaction case histories from the 2010–2011 Canterbury Earthquake Sequence: Earthquake Spectra, v. 30, p. 131–153, doi: 10.1193/030713EQS066M.

Hallegatte, S., Green, C., Nicholls, R.J., and Corfee-Morlot, J., 2013, Future flood losses in major coastal cities: Nature Climate Change, v. 3, p. 802–806, doi: 10.1038/nclimate1979.

Hanson, S., Nicholls, R., Ranger, N., Hallegatte, S., Corfee-Morlot, J., Herweijer, C., and Chateau, J., 2011, A global ranking of port cities with high exposure to climate extremes: Climatic Change, v. 104, p. 89–111, doi: 10.1007/s10584-010-9977-4.

IPCC, 2014, Climate Change 2014: Impacts, Adaptation, and Vulnerability. Part A: Global and Sectoral Aspects, *in* Field, C.B., Barros, V.R., Dokken, D.J., Mach, K.J., Mastrandrea, M.D., Bilir, T.E., Chatterjee, M., Ebi, K.L., Estrada, Y.O., Genova, R.C., Girma, B., Kissel, E.S., Levy, A.N., MacCracken, S., Mastrandrea, P.R., and White, L.L., eds., Contribution of Working Group II to the Fifth Assessment Report of the Intergovernmental Panel on Climate Change: Cambridge, UK, Cambridge University Press, 1132 p.

Kirwan, M.L., and Megonigal, J.P., 2013, Tidal wetland stability in the face of human impacts and sea-level rise: Nature, v. 504, p. 53–60, doi: 10.1038/nature12856.

McFadgen, B.G., and Goff, J.R., 2005, An earth systems approach to understanding the tectonic and cultural landscapes of linked marine embayments: Avon-Heathcote Estuary (Ihutai) and Lake Ellesmere (Waihora), New Zealand: Journal of Quaternary Science, v. 20, p. 227–237, doi: 10.1002/jqs.907.

McGranahan, G., Balk, D., and Anderson, B., 2007, The rising tide: Assessing the risks of climate change and human settlements in low elevation coastal zones: Environment and Urbanization, v. 19, p. 17–37, doi: 10.1177/0956247807076960.

Measures, R.J., and Bind, J., 2013, Hydrodynamic model of the Avon Heathcote Estuary, model build and calibration: NIWA Client Report CHC2013-116, Prepared for Environment Canterbury, 29 p.

Measures, R.J., Hicks, D.M., Shankar, U., Bind, J., Arnold, J., and Zeldis, J., 2011, Mapping earthquake induced topographical change and liquefaction in the Avon-Heathcote Estuary: NIWA Client Report CHC2011-066, Prepared for Environment Canterbury, 28 p.

Moon, L., Dizhur, D., Senaldi, I., Derakhshan, H., Griffith, M., Magenes, G., and Ingham, J., 2014, The demise of the URM building stock in Christchurch during the 2010–2011 Canterbury Earthquake Sequence: Earthquake Spectra, v. 30, p. 253–276, doi: 10.1193/022113EQS044M.

Nicholls, R.J., and Cazenave, A., 2010, Sea-level rise and its impact on coastal zones: Science, v. 328, p. 1517–1520, doi: 10.1126/science.1185782.

O'Rourke, T.D., Jeon, S.-S., Toprak, S., Cubrinovski, M., Hughes, M., van Ballegooy, S., and Bouziou, D., 2014, Earthquake response of underground pipeline networks in Christchurch, NZ: Earthquake Spectra, v. 30, p. 183–204, doi: 10.1193/030413EQS062M.

Oskin, M.E., Arrowsmith, J.R., Hinojosa Corona, A., Elliott, A.J., Fletcher, J.M., Fielding, E.J., Gold, P.O., Gonzalez Garcia, J.J., Hudnut, K.W., Liu-Zeng, J., and Teran, O.J., 2012, Near-field deformation from the El Mayor–Cucapah earthquake revealed by differential LiDAR: Science, v. 335, p. 702–705, doi: 10.1126/science.1213778.

Quigley, M., van Dissen, R., Litchfield, N., Villamor, P., Duffy, B., Barrell, D., Furlong, K., Stahl, T., Bilderback, E., and Noble, D., 2012, Surface rupture during the 2010 M_W 7.1 Darfield (Canterbury) earthquake : Implications for fault rupture dynamics and seismic-hazard analysis: Geology, p. 55–58, doi: 10.1130/G32528.1.

Quigley, M.C., Bastin, S., and Bradley, B.A., 2013, Recurrent liquefaction in Christchurch, New Zealand, during the Canterbury earthquake sequence: Geology, v. 41, p. 419–422, doi: 10.1130/G33944.1.

Shennan, I., and Hamilton, S., 2006, Coseismic and pre-seismic subsidence associated with great earthquakes in Alaska: Quaternary Science Reviews, v. 25, no. 1–2, p. 1–8, doi: 10.1016/j.quascirev.2005.09.002.

Soons, J.M., Shulmeister, J., and Holt, S., 1997, The Holocene evolution of a well-nourished gravelly barrier and lagoon complex, Kaitorete "Spit," Canterbury, New Zealand: Marine Geology, v. 138, p. 69–90, doi: 10.1016/S0025-3227(97)00003-0.

Stirling, M.W., Gerstenberger, M.C., Litchfield, N.J., McVerry, G.H., Smith, W.D., Pettinga, J., and Barnes, P., 2008, Seismic hazard of the Canterbury region, New Zealand: New earthquake source model and methodology: Bulletin of the New Zealand Society for Earthquake Engineering, v. 41, p. 51–67.

Syvitski, J.P.M., Kettner, A.J., Overeem, I., Hutton, E.W.H., Hannon, M.T., Brakenridge, G.R., Day, J., Vörösmarty, C., Saito, Y., Giosan, L., and Nicholls, R.J., 2009, Sinking deltas due to human activities: Nature Geoscience, v. 2, p. 681–686, doi: 10.1038/ngeo629.

Temmerman, S., Meire, P., Bouma, T.J., Herman, P.M.J., Ysebaert, T., and De Vriend, H.J., 2013, Ecosystem-based coastal defence in the face of global change: Nature, v. 504, p. 79–83, doi: 10.1038/nature12859.

Tonkin & Taylor, 2013, Liquefaction vulnerability study: Report for the New Zealand Earthquake Commission, February 2013, 52 p.

van Ballegooy, S., Cox, S.C., Thurlow, C., Rutter, H.K., Reynolds, T., Harrington, G., Fraser, J., and Smith, T., 2014a, Median water table elevation in Christchurch and surrounding area after the 4 September 2010 Darfield Earthquake: Version 2, GNS Science Report 2014/18, April 2014, 79 p.

van Ballegooy, S., Malan, P., Lacrosse, V., Jacka, M.E., Cubrinovski, M., Bray, J.D., O'Rourke, T.D., Crawford, S.A., and Cowan, H., 2014b, Assessment of liquefaction-induced land damage for residential Christchurch: Earthquake Spectra, v. 30, p. 31–55, doi: 10.1193/031813EQS070M.

Wang, H., Wright, T.J., Yu, Y., Lin, H., Jiang, L., Li, C., and Qiu, G., 2012, InSAR reveals coastal subsidence in the Pearl River Delta, China: Geophysical Journal International, v. 191, p. 1119–1127, doi: 10.1111/j.1365-246X.2012.05687.x.

Webster, T.L., Forbes, D.L., MacKinnon, E., and Roberts, D., 2006, Flood-risk mapping for storm-surge events and sea-level rise using LiDAR for southeast New Brunswick: Canadian Journal of Remote Sensing, v. 32, no. 2, p. 194–211, doi: 10.5589/m06-016.

Wilson, J., 1989, Christchurch—Swamp to City: A Short History of the Christchurch Drainage Board 1875–1989: Lincoln, New Zealand, Te Waihora Press, http://canterbury.royalcommission.govt.nz/documents-by-key/20110929.37 (last accessed 12 Dec. 2014).

Woodruff, J.D., Irish, J.L., and Camargo, S.J., 2013, Coastal flooding by tropical cyclones and sea-level rise: Nature, v. 504, p. 44–52, doi: 10.1038/nature12855.

Manuscript received 26 May 2014; accepted 31 July 2014. ✸